Materials Science and Engineering A 367 (2004) 82–88

MATERIALS SCIENCE & ENGINEERING A

www.elsevier.com/locate/msea

Periodic structural fluctuations during the solidification of aluminum alloys studied by neutron diffraction

N. Iqbal [a,*], N.H. van Dijk [a], V.W.J. Verhoeven [a], T. Hansen [b], L. Katgerman [c], G.J. Kearley [a]

[a] *Interfaculty Reactor Institute, Delft University of Technology, Mekelweg 15, 2629 JB Delft, The Netherlands*
[b] *ILL, 6 Rue Jules Horowitz, BP 156, 38042 Grenoble Cedex 9, France*
[c] *Laboratory for Materials Science, Delft University of Technology, Rotterdamseweg 137, 2628 AL Delft, The Netherlands*

Received 17 January 2003; received in revised form 16 September 2003

Abstract

Time-resolved neutron diffraction measurements have been carried out to study the crystallization dynamics during the liquid–solid phase transformation in an Al–0.3Ti–0.02B (wt.%) alloy. Starting from the liquid phase, the temperature was reduced to below the thermodynamic transition temperature of $T_0 = 933$ K by continuous cooling at rates of 0.6 and 0.06 K/min and by step-wise cooling in temperature steps of 1 K. After nucleation of the solid phase on the micron-size TiB_2 particles in the liquid alloy, pronounced fluctuations in the Bragg-peak intensity of the growing crystallites are observed during solidification. These fluctuations have been analyzed by a time-correlation function to extract the frequency and correlation time of the fluctuations. The deduced correlation time and oscillation frequency strongly depend on the cooling rate. The correlation time increases and the oscillation frequency decreases for decreasing cooling rate. For step-wise cooling a monotonic increase in correlation time is observed for decreasing temperatures demonstrating a slowdown of the dynamics during the liquid to solid phase transformation.

Keywords: Solidification; Aluminum alloy; Neutron diffraction; Time-correlation

1. Introduction

The understanding and control of the microscopic structure evolution during the liquid to solid phase transformation in aluminum alloys is of major importance in the modern production process of tailor-made aluminum for specific applications. Accurate investigations of the liquid structure in the neighborhood of liquid–solid phase transformation can provide useful information about the influence of the process parameters on the solidification behavior during the production process, such as cooling rate and the effect of impurities or added particles [1,2]. A significant improvement of the mechanical properties of aluminum can be obtained by the addition of small amounts of TiB_2 particles and excess titanium due to a drastic refinement of the average grain size [3]. The micrometer size TiB_2 particles enhance the nucleation rate of solid grains below the solidification temperature. The subsequent growth of nuclei is controlled by the diffusion of solute excess titanium and latent heat. A better understanding of the effects of solute titanium and added TiB_2 particles on the liquid–solid phase transformation of aluminum alloys is therefore highly desirable.

The present paper describes the neutron diffraction measurements on the temporal fluctuations in the evolution of Bragg-peak intensity during the solidification of an Al–0.3Ti–0.02B (wt.%) alloy for cooling rates of 0.06 and 0.6 K/min and for step-wise cooling. The corresponding atomic composition of this system is Al–0.16Ti–0.05B (at.%). Preliminary kinetic results of liquid structure factor and the evolution of the solid phase fraction during liquid–solid phase transformation of the same alloy have been reported elsewhere [4]. The observed temporal fluctuations can be the consequence of the ripening process between the evolving crystals in the liquid that ultimately controls the growth kinetics of these crystals. The frequency

* Corresponding author. Tel.: +31-15-278-4533; fax: +31-15-278-8303.
E-mail address: iqbal@iri.tudelft.nl (N. Iqbal).

0921-5093/$ – see front matter © 2003 Elsevier B.V. All rights reserved.
doi:10.1016/j.msea.2003.09.072

and correlation times of these temporal fluctuations during the liquid–solid phase transformation are investigated in order to obtain information on the influence of added grain refining particles on the ordering process during solidification.

2. Experimental

The sample used in this study was an Al–0.3Ti–0.02B (wt.%) alloy prepared from an Al–5Ti–0.2B (wt.%) commercial master alloy (KBM AFFILIPS). The particle size distribution of the TiB_2 precipitates in the Al–0.3Ti–0.02B alloy was determined by optical microscopy and showed particle sizes in the range from 0.6 to 2.2 μm with a maximum around 1.2 μm. The Al–0.3Ti–0.02B alloy sample with a mass of 10.6 g was placed in a cylindrical single-crystalline sapphire container with a height of 60 mm, an inner diameter of 10 mm, and a wall thickness of 1 mm.

The in situ neutron diffraction measurements were performed on the high-flux powder diffractometer D20 at the Institute Laue–Langevin (ILL). A neutron beam with a wavelength of $\lambda = 0.82$ Å and a beam height of 41 mm was used for all neutron diffraction experiments. For the high-temperature neutron diffraction measurements a dedicated vacuum furnace (7×10^{-4} mbar) was used with a vanadium heater element and a temperature stability of about 1 K. The required temperature stability ($\Delta T < 40$ mK) for our experiments was achieved with a specially designed furnace insert [4].

In order to study the solidification process of the liquid aluminum alloy three thermal treatments of Fig. 1 were applied. In all cases the Al–0.3Ti–0.02B alloy was heated to a temperature of $T = 943$ K for 1 h to obtain a homogenous liquid phase. Subsequently, the temperature was lowered to below the thermodynamic solidification temperature of $T_0 = 933$ K by continuous cooling with rates of 0.6 and 0.06 K/min and by step-wise cooling. For continuous cooling the variations in the measured structure factor were monitored in time steps of 1 min. For step-wise cooling the temperature was lowered to $T = 935$ K followed by a series of temperature steps of 1 K. The structure factor was monitored in time steps of 30 s during a period of 30 min at each temperature.

3. Results

3.1. Structure

Fig. 2 shows the measured structure factor S(Q) of the Al–0.3Ti–0.02B alloy in the pure liquid and pure solid state. Where $Q = (4\pi/\lambda)\sin(\theta)$ is the wave vector transfer with 2θ as the scattering angle, and λ is the neutron wavelength. The intensity of the solid phase is scaled to the maximum intensity of (1 1 1) Bragg-peak. The first peak in the liquid structure factor of Al–0.3Ti–0.02B alloy is observed at $Q = 2.68$ Å^{-1} and has a height of S(Q) = 2.39. In addition, a small peak in the liquid structure factor of the Al–0.3Ti–0.02B alloy is observed below the first liquid peak. This additional peak at $Q = 1.95$ Å^{-1} corresponds to a (0 0 1) Bragg reflection of the solid TiB_2 particles with a hexagonal crystal lattice structure in the liquid alloy. During the liquid to solid phase transformation, the liquid peaks in the structure factor gradually decrease while the Bragg peaks from the solid phase with a face-centered cubic lattice structure ($a = 4.14$ Å) emerge. The observed relative Bragg-peak intensities deviate significantly from the expected powder average indicating the presence of texture. In the following discussion the height of the first liquid peak at $Q = 2.68$ Å^{-1} is used to deduce the value of liquid phase fraction f_L and the corresponding value of solid fraction $f_S = 1 - f_L$. During liquid to solid phase transformation the change in solid fraction f_S is deduced from the normalized variation in the height of first peak in the liquid structure factor S(Q). As the position and the width of the first liq-

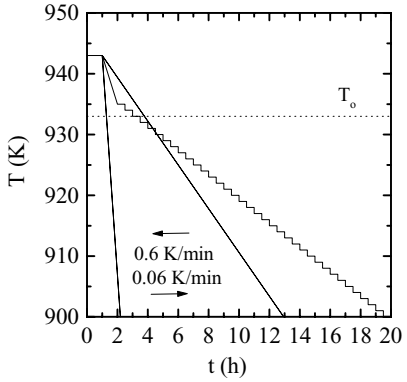

Fig. 1. Temperature profiles for solidification experiments for Al–0.3Ti–0.02B alloy with cooling rate of 0.06 and 0.6 K/min and with step-wise cooling.

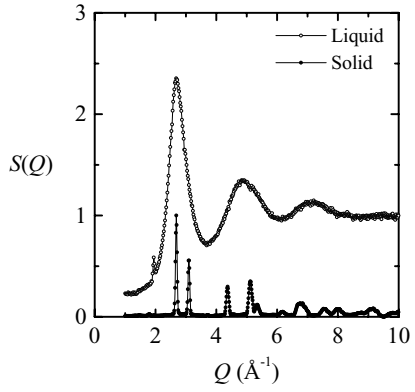

Fig. 2. Structure factor of the Al–0.3Ti–0.02B alloy, in the liquid (open circles) and in the solid state (solid circles).

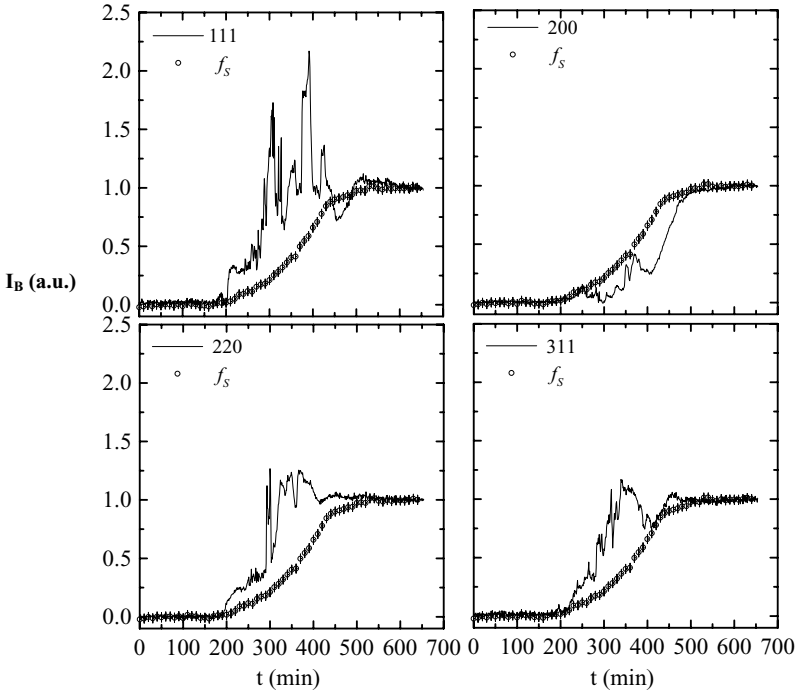

Fig. 3. Time evolution of the normalized intensities of the main Bragg peaks for the Al–0.3Ti–0.02B alloy (solid line) and solid fraction $f_S = 1 - f_L$ (open circles) at a cooling rate of 0.06 K/min.

uid peak does not change significantly during solidification, this is equivalent to an integration over the first liquid peak. Such an integration would however require a separation of the contributions of the liquid and the solid phase to the structure factor and is therefor more sensitive to systematic errors.

3.2. Solidification kinetics

In Fig. 3 the solid fraction f_S is compared to the relative variation in the monitored Bragg reflections of the solid phase I_B during the continuous cooling of the Al–0.3Ti–0.02B alloy at a rate of 0.06 K/min. The transformation kinetics of the solid-phase fraction as a function of the cooling rate is discussed in detail in [4]. During the transformation of the Al–0.3Ti–0.02B alloy a remarkable oscillatory growth of Bragg-peak intensity is observed for the integrated intensity of the (1 1 1), (2 0 0), (2 2 0), and (3 1 1) reflections. It is interesting to note that the oscillations are observed only in the Bragg-peak intensity and not in the solid volume fraction. Further, there is no direct correlation observed in the fluctuations between the Bragg intensity of the monitored reflections. This oscillatory behavior of Bragg-peak intensity appears to be intrinsic to the material under study. In Fig. 4 the intensity evolution of Bragg peaks and the corresponding solid fraction f_S is shown for a continuous cooling rate of 0.6 K/min. Again the evolution of the Bragg-peak intensity shows an oscillatory behavior. As expected, the oscillations observed at a cooling rate of 0.6 K/min are however, less pronounced than for the cooling rate of 0.06 K/min.

4. Discussion

In order to study the kinetics of the solidification process the Johnson–Mehl–Avrami (JMA) model [5–8] is applied. According to the JMA model the functional form for the ordered volume fraction $f(t)$ as a function of time t is predicted to be

$$f(t) = 1 - \exp\{-k(t - t_0)^n\} \quad (1)$$

where k is the rate constant, t_0 is the incubation time, and n the Avrami exponent. The value of the exponent n is expected to vary between 1 and 4 depending on the nucleation mechanism and the growth dimensionality [9]. In Fig. 5a, the growth of (1 1 1) Bragg-peak intensity and the fit of the experimental data to JMA equation is shown as a function of time for the cooling rate of 0.06 K/min. A reasonable fit to the experimental data was obtained for $n = 3$, corresponding to a three-dimensional (3D) grain growth of existing nuclei [4]. Fig. 5b shows the temporal fluctuations in the (1 1 1), (2 0 0), (2 2 0), and (3 1 1) Bragg-peak intensity for cooling rates of 0.06 K/min after subtraction of the fit with the JMA model $\Delta I_B(t) = I_B(t) - I_{JMA}(t)$. During the solidification process the fluctuations in the relative Bragg-peak intensity are significantly larger than the statistical noise in the pure solid and pure liquid phases.

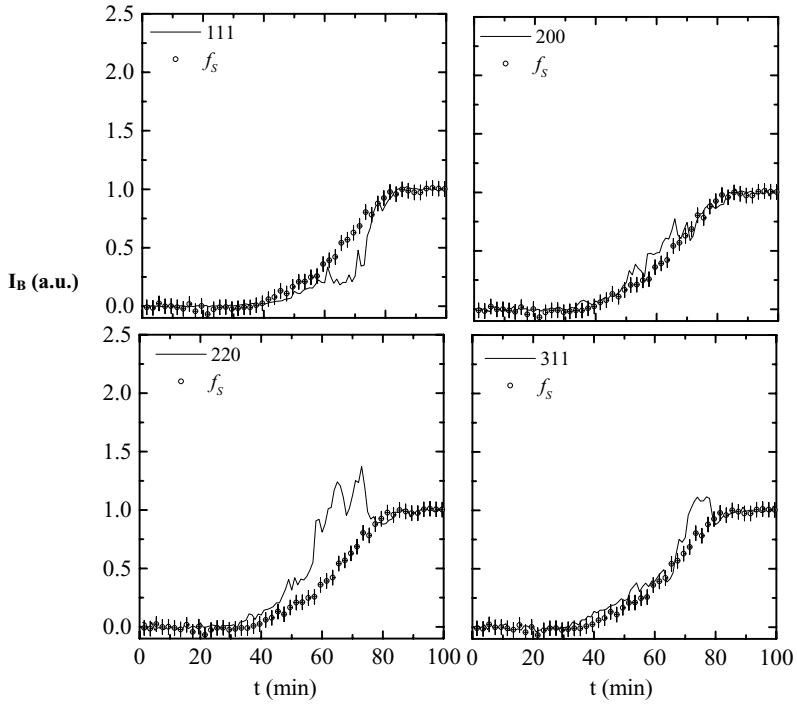

Fig. 4. Time evolution of the normalized intensities of the main Bragg peaks for the Al–0.3Ti–0.02B alloy (solid line) and solid fraction $f_S = 1 - f_L$ (open circles) at a cooling rate of 0.6 K/min.

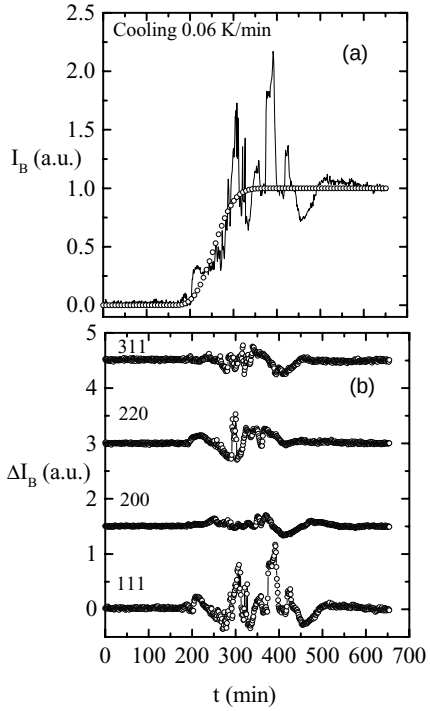

Fig. 5. Time evolution of (a) the normalized intensity of the (1 1 1) Bragg peak for the Al–0.3Ti–0.02B alloy (solid line) at a cooling rate of 0.06 K/min. The open circles indicate a fit to the data with the Johnson–Mehl–Avrami model (see text). (b) The temporal fluctuations in the relative Bragg peaks ($\Delta I_B = I_B - I_{JMA}$) for the Al–0.3Ti–0.02B alloy at a cooling rate of 0.06 K/min.

For the time-dependent measurements with a constant sampling time, Δt, the fluctuations in the relative Bragg-peak intensity, $\Delta I_B(t)$, can be analyzed in terms of the normalized time-correlation function [10]

$$g^{(2)}(\tau) - 1 = \frac{\frac{1}{M}\sum_{i=0}^{M}[\Delta I_B(t_i) - \langle \Delta I_B \rangle][\Delta I_B(t_i + \tau) - \langle \Delta I_B \rangle]}{\frac{1}{N}\sum_{i=0}^{N}[\Delta I_B(t_i) - \langle \Delta I_B \rangle]^2} \quad (2)$$

where τ is the time difference, $\langle \Delta I_B \rangle$ the time-averaged relative Bragg-peak intensity. The values of $N = t_{trans}/\Delta t$ are determined by the ratio between the transformation time t_{trans} and the sampling time Δt. For the continuous cooling experiments $N = 656$ and 102 were used for the cooling rates of 0.06 and 0.6 K/min, respectively. For the step-wise cooling a constant value of $N = 59$ was used for all steps. The sampling time Δt amounts to 1 min for the continuous cooling measurements and 30 s for the step-wise cooling measurements. The value of M vary between 0 and N, according to the relation $M = N - \tau/\Delta t$. The calculated time-correlation function of the relative Bragg-peak intensity is shown in Figs. 6a and 7a for the cooling rates of 0.06 and 0.6 K/min, respectively. The Fourier transform of the time-correlation functions at cooling rates of 0.06 and 0.6 K/min are shown in Figs. 6b and 7b. The results of Fourier transforms (FFT) of the time-correlation function clearly indicate that there are pronounced peaks that evidence the existence of non-random oscillations. For a random signal the normalized time-correlation function corresponds to $g^{(2)}(\tau) - 1 = \delta(\tau)$, while for correlated signals

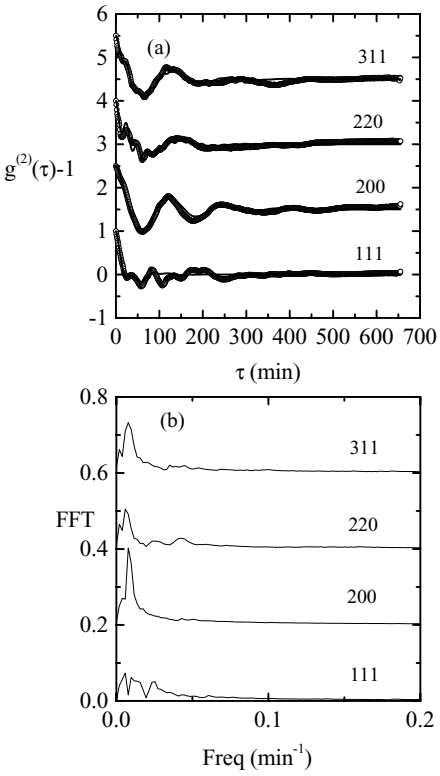

Fig. 6. Normalized time-correlation function for the (1 1 1), (2 0 0), (2 2 0), and (3 1 1) reflections for a cooling rate of 0.06 K/min (a) and its Fourier transform (b). The solid line in (a) is a fit to Eq. (3). For clarity each curve is displaced by 1.5 in (a) and 0.2 in (b) compared to immediate lower curve.

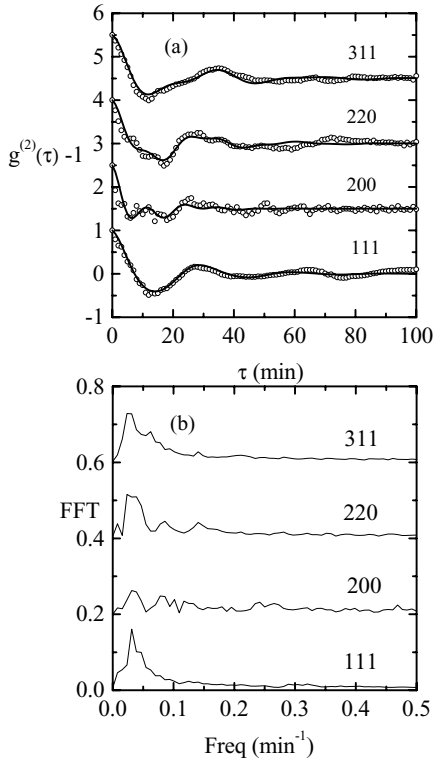

Fig. 7. Normalized time-correlation function for the (1 1 1), (2 0 0), (2 2 0), and (3 1 1) reflections for a cooling rate of 0.6 K/min (a) and its Fourier transform (b). The solid line in (a) is a fit to Eq. (3). For clarity curve for each reflection is displaced by 1.5 in (a) and 0.2 in (b) compared to immediate lower curve.

it can be described in terms of a series of damped oscillations. In order to model the time-correlation functions we have limited the number of oscillation frequencies to two and assume the following form:

$$g^{(2)}(\tau) - 1 = \exp\left(-\frac{\tau}{\tau_c}\right)[A\cos(\omega_1\tau) + (1-A)\cos(\omega_2\tau)] \quad (3)$$

where A is a constant weighing factor, τ_c is the fitted time constant, ω_1 and ω_2 are the oscillation frequencies. The fitted time-correlation function for cooling rates of 0.06 and 0.6 K/min. are shown in Figs. 6a and 7a. The parameters A, τ_c, ω_1 and ω_2 obtained by fitting the time-correlation function to Eq. (3), are listed in Table 1 for all the four Bragg reflection and for cooling rates of 0.06 and 0.6 K/min. The results indicate that the correlation time and oscillation frequencies are of the same order of magnitude for the (1 1 1), (2 0 0), (2 2 0), and (3 1 1) Bragg reflections at a given cooling rate but strongly depend on the cooling rate. The damping time increases and the oscillation frequencies decrease for a decreasing cooling rate.

The time-correlation functions were also determined for the step-wise cooling measurements of Fig. 1 at each of the constant temperatures. At each temperature the Bragg-peak intensity was monitored for 30 min at a sampling rate of 30 s. Fig. 8 shows the change in solid fraction f_S and the corresponding normalized Bragg-peak intensity I_B for the (1 1 1) reflection, as a function of temperature. As observed for continuous cooling, pronounced oscillations are observed in time-correlation function at constant temperatures during stepwise cooling. These oscillations can be fitted with a damped periodic function with a single frequency in Eq. (3) and $A = 1$. The fitted temperature-dependent correlation time τ_c and oscillation frequency ω are given in Fig. 9. The correlation time is found to increase for decreasing temperature with the maximum value of 152 min at a temperature of $T = 906$ K.

The physical origin of these quasi-periodic, temporal fluctuations in the Bragg-peak intensity, is a matter of some speculation. There are three different mechanisms that can in principle be responsible for the observed time fluctuations: crystallite motion, Ostwald ripening and growth fluctuations.

The first scenario for the interpretation of the observed temporal oscillations in the Bragg-peak intensity arises from a limited number of grains in the irradiated sample volume. In the absence of a true powder average, the fluctuations in the Bragg-peak intensity may be caused by the random motion of solid grains in the liquid. This interpretation seems unlikely due to the quasi-periodic nature of oscillations and

Table 1
Time constants τ_c (a); oscillation frequency ω_1 and ω_2 (b); and amplitude A (c) for the temporal fluctuations in the Bragg-peak intensity of the (1 1 1), (2 0 0), (2 2 0), and (3 1 1) crystal reflections of the Al–0.3Ti–0.02B alloy at two different cooling rates

Cooling rate (K/min)	τ_c (min)				
	(1 1 1)	(2 0 0)	(2 2 0)	(3 1 1)	
(a)					
0.06	35(2)	105(2)	69(2)	84(2)	
0.60	19(1)	12(1)	20(1)	23(1)	
Cooling rate (K/min)	Frequency (min^{-1})	(1 1 1)	(2 0 0)	(2 2 0)	(3 1 1)
(b)					
0.06	ω_1	0.056(1)	0.050(2)	0.040(4)	0.050(2)
	ω_2	0.151(2)	0.198(5)	0.25(1)	0.24(2)
0.60	ω_1	0.208(2)	0.21(1)	0.21(1)	0.189(2)
	ω_2	0.45(4)	0.53(1)	0.52(2)	0.34(1)
Cooling rate (K/min)	A				
	(1 1 1)	(2 0 0)	(2 2 0)	(3 1 1)	
(c)					
0.06	0.68(1)	0.96(1)	0.70(1)	0.87(1)	
0.60	0.94(2)	0.50(4)	0.77(3)	0.70(2)	

The parameters were obtained from a fit of the correlation function of the normalized variations in the Bragg-peak intensity to Eq. (3).

the limited mobility of relatively massive grains. For the current beam size of 1 cm × 4.1 cm, sample diameter of 1 cm, and an estimated grain size of 640 and 460 μm in solid material for cooling rates of 0.06 and 0.6 K/min, one would expect to see the scattering from the order of 10^5 grains. Estimates from the absolute value of the (1 1 1) Bragg-peak intensity suggests an average number of $N \approx 3.0 \times 10^2$ and 1.8×10^3 grains in reflection for cooling rates of 0.06 and 0.6 K/min, respectively. Then assuming finite size effects, the intensity fluctuations will be of the order of $1/\sqrt{N}$, which is too small compared to observed oscillations. Therefore this process does not explain the quasi-periodic nature nor the amplitude of observed intensity fluctuations.

A ripening process is expected to play a significant role for the slow cooling rates applied in our experiment. Each

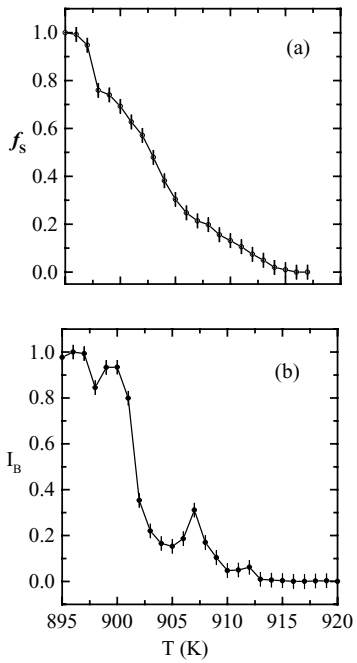

Fig. 8. The solid fraction f_S (a) and the Bragg-peak intensity of the (1 1 1) reflection (b) as a function of temperature during step-wise cooling.

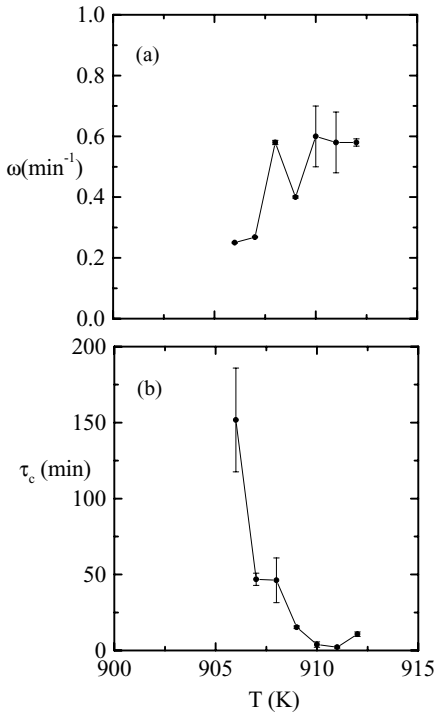

Fig. 9. The oscillation frequency ω (a) and the time constant τ_c (b) determined from the normalized time-correlation function as a function of temperature for the (1 1 1) Bragg peak, during stepwise cooling.

of the final crystallites in the Al–0.3Ti–0.02B alloy contains a large number of TiB_2 nucleating particles. This may indicate that during the growth of the crystallites nucleated by the grain refiners a significant interaction among the crystallites through the Ostwald ripening takes place so as to reduce the system interface energy. During this process a grain can grow at the expense of some of its neighbors, although at the same time it may be consumed by other neighbors, maintaining the local equilibrium. This can result in the quasi-periodic intensity fluctuations of Bragg peaks to which they are reflecting. This continues until the grain size distribution is relaxing to its steady state. As the solidification proceeds and the average crystallites grow in size this process is expected to slow down as observed in the step-wise cooling experiments shown in Fig. 9.

The last scenario corresponds to growth fluctuations and can be caused by local fluctuations in temperature (or alternatively in alloy concentration). During the crystallite growth latent heat is released leading to local temperature variations that can subsequently slow down the growth rate. Although this process can be responsible for fluctuations in the increase of the Bragg-peak intensity it is unlikely that it can lead to temporary decreases as experimentally observed.

We therefore consider the second scenario of Ostwald ripening as the most plausible mechanism responsible for temporal growth variations, which provides a qualitative explanation of the non-random oscillations observed during solidification of the Al–0.3Ti–0.02B alloy.

5. Conclusions

We have presented experimental data on the crystallization dynamics during the liquid–solid phase transformation in an Al–0.3Ti–0.02B alloy, as a function of cooling rate and temperature. It is found that oscillations in the Bragg-peak intensities are observed during the liquid–solid phase transformation, which have a non-random character. The average correlation time and the oscillation frequency is found to be dependent on the cooling rate. The time constant increases and the oscillation frequency decreases for a decreasing cooling rate. The origin of these oscillations seems likely to be the ripening interaction among the evolving crystals that ultimately controls the grain growth. Stepwise cooling measurements further indicate a slow down in the crystallization dynamics for decreasing temperatures, suggesting that the ripening process saturates as the crystals grow in size below the transition temperature.

Acknowledgements

We thank the Institute Laue–Langevin for the beam time to perform these neutron diffraction experiments. This work was financed in part by The Netherlands Foundation for Fundamental Research of Matter (FOM) and The Netherlands Institute for Metals Research (NIMR).

References

[1] R.F. Shannon, M.G. Glavicic, M.A. Singh, J. Macromol. Sci. B 33 (1994) 357.
[2] C.M. Allen, K.A.Q. O'Reilly, B. Cantor, P.V. Evans, Mat. Sci. Eng. A 226–228 (1997) 784.
[3] M. Easton, D. Stjohn, Met. Mater. Trans. A 30 (1999) 1625.
[4] N. Iqbal, N.H. van Dijk, V.W.J. Verhoeven, W. Montfrooij, T. Hansen, L. Katgerman, G.J. Kearley, Acta Mater. 51 (2003) 4497.
[5] J. Johnson, R. Mehl, Trans. AIME 135 (1939) 416.
[6] M. Avrami, J. Chem. Phys. 7 (1939) 1103.
[7] M. Avrami, J. Chem. Phys. 8 (1940) 212.
[8] M. Avrami, J. Chem. Phys. 9 (1941) 177.
[9] D.W. Henderson, J. Therm. Anal. 15 (1979) 325.
[10] H.Z. Cummins, E.R. Pike, Photon Correlation Spectroscopy and Velocimetry, Plenum Press, New York, 1977.